

BCSJ Award Article

The Self-Assembly of Amphiphilic Oligothiophenes: Hydrogen Bonding and Poly(glutamate) Complexation

Fiorella Brustolin,[1] Mathieu Surin,[2] Vincent Lemaur,[2] Giuseppe Romanazzi,[3] Qianyao Sun,[1] Jérôme Cornil,[2] Roberto Lazzaroni,[2] Nico A. J. M. Sommerdijk,[1] Philippe Leclère,*[1,2] and E. W. Meijer*[1]

[1]Laboratory for Macromolecular and Organic Chemistry, Eindhoven University of Technology, P. O. Box 513, 5600 MB Eindhoven, The Netherlands

[2]Laboratory for Chemistry of Novel Materials, University of Mons-Hainaut, B-7000, Mons, Belgium

[3]Department of Water Engineering and Chemistry (DIAC), Polytechnic of Bari, via Orabona 4, I-70125 Bari, Italy

Received March 12, 2007; E-mail: e.w.meijer@tue.nl

The self-organization behavior of an amphiphilic sexithiophene bearing amide functionalities is studied and compared to that of a derivative bearing an ester group at the same position. The introduction of hydrogen-bond interactions in assemblies of these π-conjugated oligomers is found to affect the molecular organization both in protic media and in thin deposits on mica. The amphiphilic 2,2′;5′,2″;5″,2‴;5‴,2⁗;5⁗,2⁗′-sexithiophene-5,5⁗′-dicarboxylic acid bis[(4,7,10,13,16-pentaoxaheptadecyl)amide] forms assemblies in *n*-butanol and water and partially aggregates in toluene. Spectroscopy reveals that the presence of a hydrogen-bonding moiety increases the thermal stability of the assemblies in *n*-butanol and even more in water solution. On mica surfaces, the formation of rod-like one-dimensional nanostructures is observed after deposition from toluene solutions. In addition, transmission electron microscopy in combination with selected area electron diffraction shows that in water plate-like structures are formed built from parallel oriented stacks, with a π–π distance of 3.5 Å. Comparison of these data to molecular modeling and quantum chemistry calculations is used to better understand the influence of the amide group on the stacking of these compounds. The introduction of these H-bonding interactions leads to denser and more stable stacks. Furthermore, we show that a derivative of the amide compound, bearing terminal ammonium groups, forms a complex with chiral polyanions in aqueous media such that the sexithiophene segments are stacked in a meta-stable helical fashion with preferred handedness. We observed that poly(glutamate) and DNA generate a chiral sexithiophene assembly. In time the induced chirality disappears, which is explained by the meta-stability of the kinetically formed adduct. This constitutes one step forward towards the controlled formation of functional multi-component systems in aqueous solution.

The possibility to generate materials with improved electronic properties by controlling the molecular organization of conjugated polymers and oligomers has been driving the design of self-assembling π-conjugated materials for several years now.[1] In particular, the pre-organization of well-defined oligomeric systems such as α,ω-disubstituted sexithiophene derivatives has been demonstrated as a promising approach to conjugated materials with a high degree of spatial orientation and packing of the constituent building blocks.[2] In this context, the possibility of organizing these materials via assembly in aqueous media has recently attracted attention, leading to the design of amphiphilic π-conjugated systems.[3] This is exemplified by the formation of aggregates from sexithiophenes bearing oligo(ethylene oxide)-substituted end groups[4] (**2**, Chart 1) or cationic end groups[5] and oligo(*p*-phenylenevinylene) (OPV) and others with oligo(ethylene oxide)[6] or sulfonic acid[7] side groups, in which hydrophobic interactions have been utilized as the driving force for the formation of the assemblies.

The induction of helical order in conjugated polymers has been achieved, e.g., through the interplay of supramolecular and ionic interactions of enantiopure low molecular weight compounds with various polymer side chains,[8] and through the synthesis of poly(acetylene)s within a chiral nematic liquid-crystalline phase.[9] In contrast, the construction of helical assemblies of π-conjugated oligomers has been mainly accomplished through the use of intrinsically chiral building blocks[10] or via "Sergeant-and-Soldiers" effects[11] and only

Published on the web September 13, 2007; doi:10.1246/bcsj.80.1703

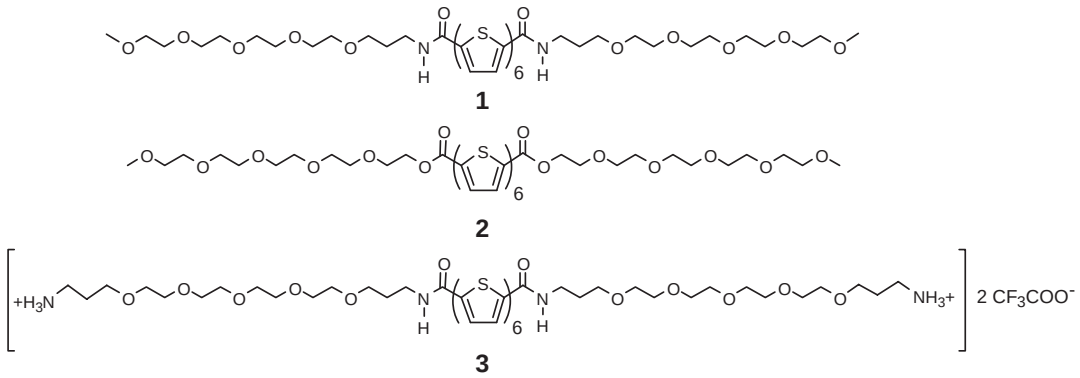

Chart 1.

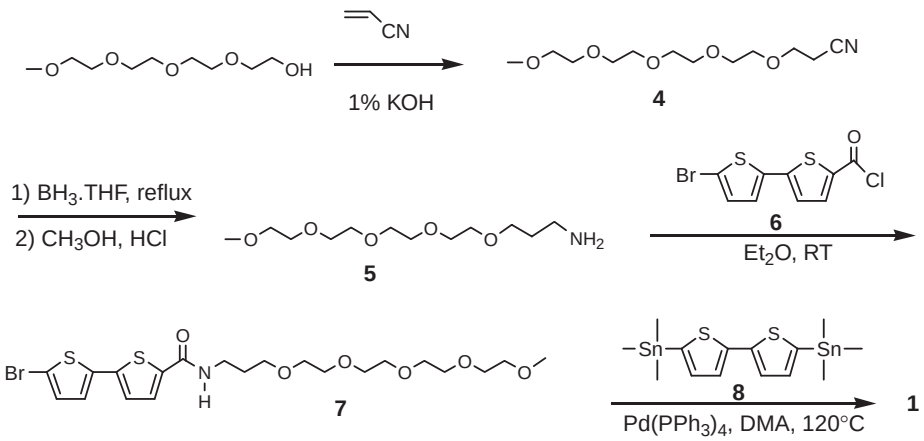

Scheme 1.

few examples exist in which helicity is generated through induction by solvents or other chiral molecules.[12,13] Since it has been long demonstrated that the use of hydrogen-bonding moieties can improve the positional order of component molecules, e.g., in surfactant aggregates,[14] low molecular weight organogels[15–17] and liquid-crystalline discotics,[18,19] we designed two amphiphilic oligomers **1** and **3** (Chart 1) consisting of a sexithiophene unit end-capped by two oligo(ethylene oxide) chains that are linked to the heteroaromatic core by amide bonds. These are expected to lead to the formation of a hydrogen-bond motif that directs and stabilizes the ordered assembly and the resulting π–π stacking imposed by the hydrophobic interactions of **1** and **3** in polar protic media.

The possibilities of organizing π-conjugated oligomers were further extended by the introduction of a terminal ammonium group in the oligo(ethylene oxide) chains (**3**). This allows the possibility of complexation with chiral anionic macromolecules and thereby the introduction of helical order in the assemblies of such oligomers. Here, we show how the complexation with poly(glutamate) gives rise to a templating interaction that assembles the molecules of **3** such that the chirality of the polymer is reflected in the organization of the stacks. These results may bear implications for the application of π-conjugated materials in the molecular recognition of biomacromolecules.[9b–e,20,21]

Results and Discussion

Synthesis. Sexithiophene **1** was synthesized from 5′-bromo-2,2′-bithiophene-5-carbonyl chloride (**6**),[4] which was reacted with amine **5** to give the asymmetrically substituted bithiophene **7** (Scheme 1). Amine **5** was obtained through a Michael addition of tetra(ethylene glycol) mono methyl ether on acrylonitrile in the presence of KOH yielding **4**, the latter was reduced to the corresponding amine with $BH_3 \cdot$THF. Subsequently, two equivalents of **7** were coupled with 5,5′-bis(trimethylstannyl)-2,2′-bithiophene (**8**) in the presence of a catalytic amount of tetrakis(triphenylphosphine)palladium(0) in dimethylacetamide (DMA). The synthesis of sexithiophene **2** was published before.[4b] Sexithiophene **3** was synthesized following the procedure as described in Scheme 2. 5′-Bromo-2,2′-bithiophene-5-carbonyl chloride (**6**)[4b] was reacted with the mono-protected amine **11** to give the asymmetrically substituted bithiophene **12**. The synthesis of mono Boc-protected amine **11** proceeded from a Michael addition of tetraethylene glycol on acrylonitrile in the presence of KOH to give the symmetrical product **9**, which was reduced to the corresponding diamine **10** with $BH_3 \cdot$THF. Reaction with di-*tert*-butyl dicarbonate yielded the mono-protected product **11** in 68% yield; the difference in solubility of the mono-, non-, and double-protected product made separation easy. Subsequently, 5,5′-bis(trimethylstannyl)-2,2′-bithiophene (**8**)[42] was reacted with two

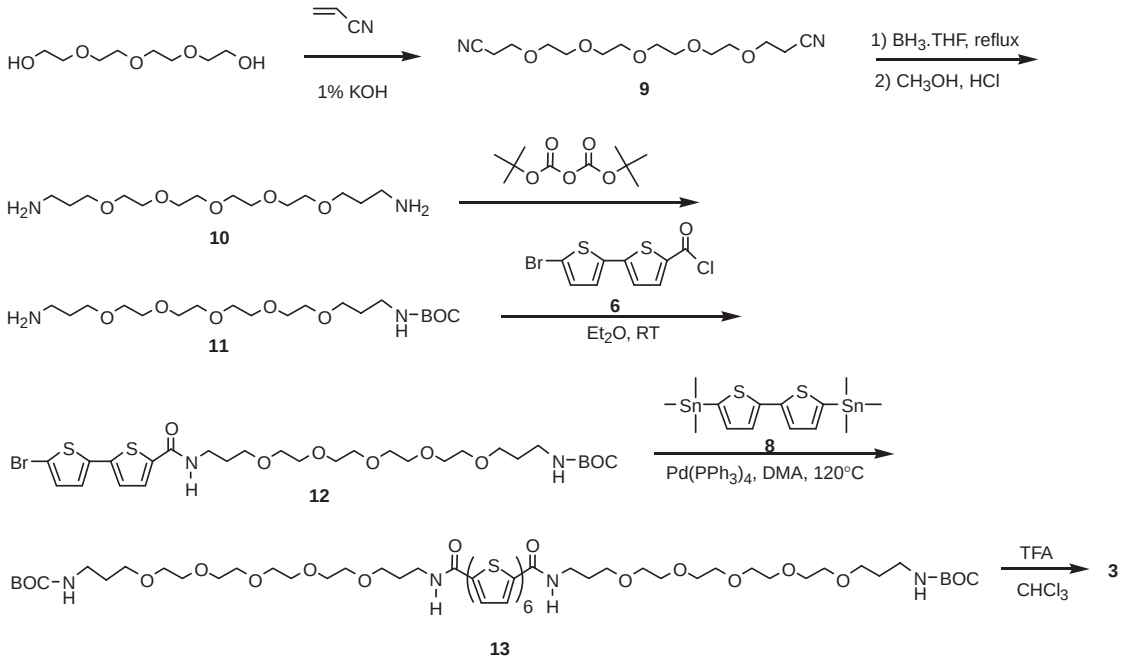

Scheme 2.

equivalents of **12** in the presence of a catalytic amount of tetrakis(triphenylphosphine)palladium(0) in DMA giving **13** in 50% yield. Deprotection of **13** with trifluoroacetic acid (TFA) yielded the desired bisammonium salt **3** in 100% yield.

Self-Organization in Solution and at Surfaces. In dilute chloroform solutions ($\approx 10^{-5}$ M), **1** displays a UV–vis absorption band with a maximum at $\lambda_{max} = 435$ nm, typical for molecularly dissolved sexithiophene chromophores (Fig. 1a). In support of this, the corresponding fluorescence spectrum reveals a structured broad band at $\lambda_{max} = 520$ with a shoulder at $\lambda_{max} = 550$ nm, also pointing to the presence of isolated oligomer molecules in solution (Fig. 1b).

^{1}H NMR shows that upon going to higher concentrations ($>10^{-3}$ M) a downfield shift from 7.16 to 7.24 ppm is observed for the signal associated with the amide proton, along with an upfield shift of the sexithiophene proton resonances of $\approx$0.1 ppm (Fig. 1b). The shifts are attributed to the formation of assemblies in which hydrogen bonds between the amide groups, in tandem with π–π interactions, lock the aromatic cores on top of one another. Since no concomitant line broadening is observed in the sexithiophene resonances, it is deduced that a high local mobility is still present and that the observed shifts are probably the result of the onset of aggregation.

When films are prepared by drop-casting a dilute chloroform solution onto mica substrates, the UV–vis spectra of these films show a remarkable blue-shift of the absorption band to 390 nm and the appearance of a vibronic progression, whereas fluorescence spectra display an emission band at $\lambda_{max} = 607$ nm with a shoulder at $\lambda_{max} \cong 630$ nm (Fig. 2), both pointing to the formation of aggregates[22,23] of **1** in the solid state. Where 3-substituted oligo- and polythiophenes typically show a red shift on aggregation, non-substituted or ω–ω' substituted oligothiophenes show a blue shift on aggregation. The specific packing and exciton coupling with favored probability of the highest energy transition explains this blue shift. The stability of these aggregates is illustrated by the fact that upon heating these films to 150 °C no spectral changes are observed. AFM reveals that these films are discontinuous and consist of interconnected islands with a uniform thickness of $\approx$6 nm (Fig. 3a). This value corresponds to the length of the molecule which indicates that the observed solid-state assembly is not guided by molecule-surface interaction with the substrate but more interaction between molecules themselves (see below). Therefore, we tentatively suggest that aggregates are formed at an early stage during solvent evaporation with the molecules standing up within the aggregates.

When **1** is deposited on mica from toluene solutions, AFM revealed besides the presence of large aggregates with no distinct morphologies also the formation of rod-like structures with lengths from 200–500 nm and widths of $\approx$6 nm (after correction, see Experimental Section), which are oriented according to the three-fold symmetry of the mica substrate (Figs. 3b and 3c). Inspection of a molecular model indicates that the width of the observed structures is consistent with the formation of one-molecule-wide stacks based on the overlap of the heteroaromatic cores. Correspondingly, the broad UV–vis absorption spectrum indicates that in toluene **1** is present as a mixed population of aggregated and molecularly dissolved states (Fig. 4). After a few days, the absorption band at $\lambda_{max} =$ 395 nm becomes even more predominant, indicating that in time molecules of **1** form more or larger aggregates in this solution, this is in marked contrast to the solution behavior of **2** which does not aggregate in toluene.[4a] A similar difference is observed in THF solution, which is also a good solvent for **2**. It is likely that the presence of the amide groups in **1** is responsible for this enhanced tendency of these molecules to aggregate.

We propose that the observed rod-like aggregates are

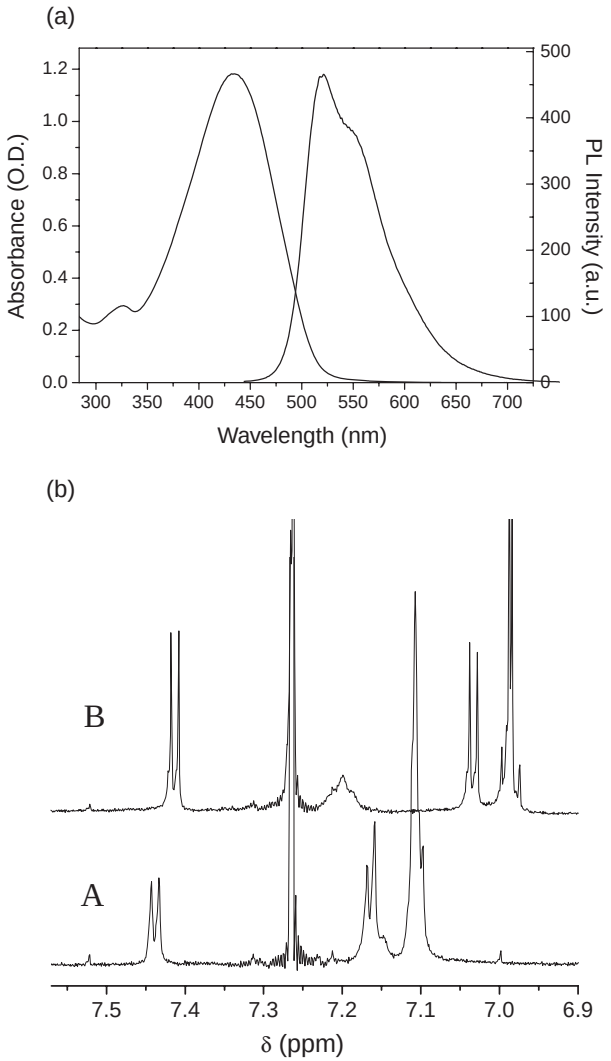

Fig. 1. (a) UV–vis and fluorescence spectra of **1** in chloroform. Concentration: $2.5 \cdot 10^{-5}$ M (UV), $2.5 \cdot 10^{-6}$ M (PL). (b) ^{1}H NMR spectra of **1** in $CDCl_3$ for a dilute solution (A) and for concentrations higher than 10^{-3} M (B).

formed from the molecularly dissolved material; the relatively slow evaporation rate of toluene may be a key factor in controlling their shape and orientation, as this allows a higher degree of interaction with the mica surface during the growth of the assemblies. The importance of the amide groups in the formation of these nanostructures is demonstrated again by comparison with the corresponding sexithiophene-based ester derivative **2**, that only shows the formation of islands when deposited onto mica from the same solvent.[24,25] This difference is tentatively attributed to the possibility of **1** to form arrays of hydrogen bonds that rigidify and structure the aggregates.

When dissolved in *n*-butanol at room temperature, **1** showed an absorption maximum at $\lambda_{max} = 390$ nm, indicating the presence of aggregates as the predominant species, even in dilute solutions (Fig. 5a).[26] The fluorescence in this state concomitantly shows a considerable quenching (compared to chloroform solutions) of the emission bands at $\lambda_{max} = 520$ and 550 nm and now revealed a contribution of the aggregated state at $\lambda_{max} \approx 600$ nm.[4]

Variable-temperature UV–vis spectroscopy reveals that upon heating from -10 to 90 °C a transition occurs at 72 °C

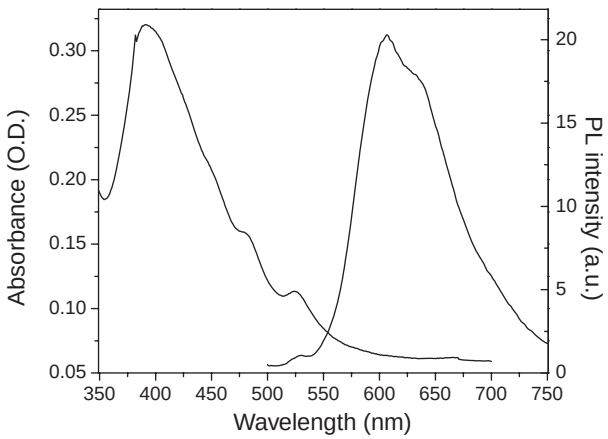

Fig. 2. UV–vis and fluorescence spectra of a film of **1** drop-cast from chloroform.

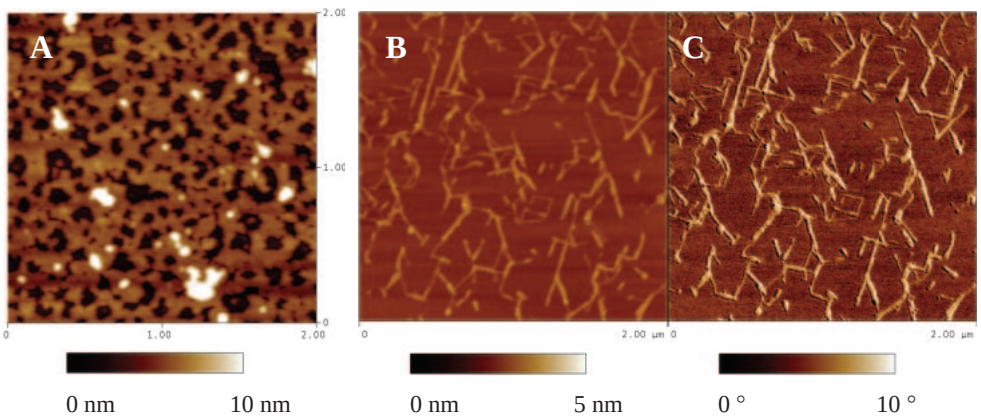

Fig. 3. (A) $2 \times 2\,\mu m^2$ AFM tapping-mode topographic image of **1** deposited from chloroform on a mica substrate. (B) $2 \times 2\,\mu m^2$ AFM tapping-mode topographic (C) and phase images of **1** deposited from toluene on a mica substrate.

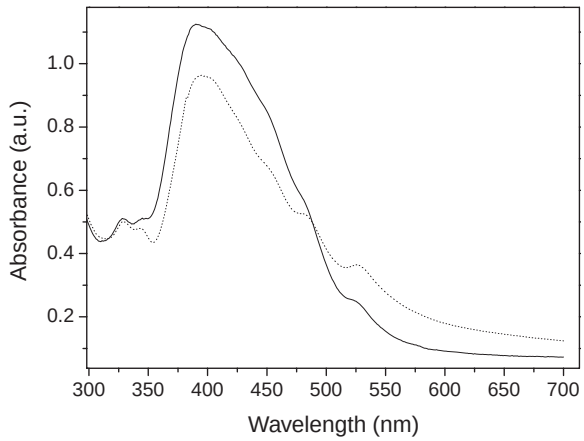

Fig. 4. UV–vis spectrum of **1** in toluene ($2\cdot10^{-5}$ M) for a freshly prepared solution (solid line) and for the same solution after a few days (dotted line, normalized intensities).

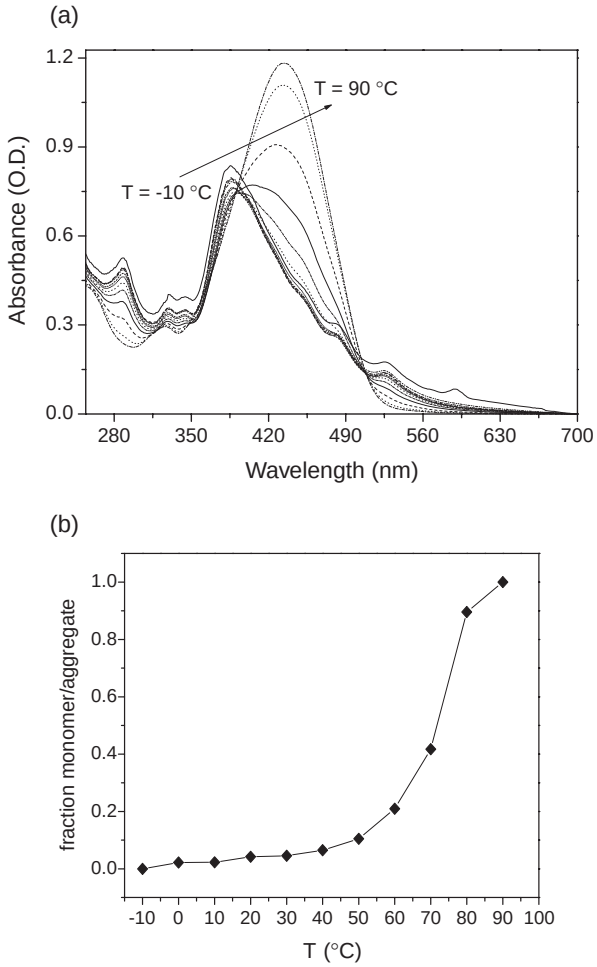

Fig. 5. (a) UV–vis spectra of **1** in *n*-butanol ($2.5\cdot10^{-5}$ M) as a function of temperature (temperature range: −10–90 °C). (b) Normalized aggregate/monomer ratio versus temperature obtained from UV–vis data of **1** in *n*-butanol.

(Fig. 5b) from the aggregated to the molecularly dissolved state as evidenced by the increase of the adsorption band at $\lambda_{max} = 435$ nm, the concomitant decrease of the band at

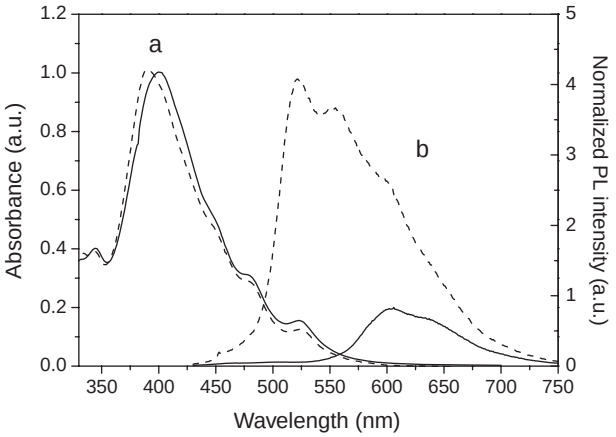

Fig. 6. UV–vis (a, solid line) and fluorescence (b, solid line) spectra of **1** in water recorded at room temperature (UV: $3.6\cdot10^{-5}$ M, PL: $3.6\cdot10^{-6}$ M). For comparison, UV–vis (a, dashed line) and fluorescence (b, dashed line) spectra of **1** in *n*-butanol are also shown (normalized intensities).

$\lambda_{max} = 390$ nm and the observation of a clear isosbestic point (Fig. 5a). The fact that in the present case the transition point is observed at a temperature approximately 20 °C higher than for the ester derivative **2**[4] demonstrates that the presence of amide moieties is an important factor not only for the formation but also for the stabilization of these aggregates.

By injecting a freshly sonicated THF solution of **1** into water at room temperature and subsequently removing the organic solvent, a clear aqueous solution was obtained. UV–vis spectroscopy revealed an asymmetric, structured absorption of the π–π transition with a maximum at $\lambda_{max} = 400$ nm, clearly pointing to the presence of aggregates of **1** in water (Fig. 6). The fluorescence spectrum in this case displays exclusively a low energy emission at 603 nm, indicating that in water aggregates are the only emitting species (Fig. 6). The observed red shift of ≈20 nm in the emission with respect to the value observed for **2** in the same solvent suggests that, in these aggregates, the oligomers are more closely packed compared to the ester derivative due to the involvement of hydrogen-bonding interactions. This hypothesis is supported by the increased stability of the aggregates in the aqueous medium, which show no thermal transition to isolated molecules in the temperature range from 0–90 °C, apart from a small blue-shift of the absorption maximum.

AFM in combination with transmission electron microscopy (TEM) indeed demonstrate the presence of plate-like aggregates with dimensions ranging from 100–500 nm (Fig. 7a) and a height of 2.8 nm.[27] More importantly, selected area electron diffraction reveals for these aggregates a *d*-spacing of 3.5 Å along a single direction in the plates (Fig. 7b). This not only confirms the tight packing of the molecules, but it can also be inferred that the resulting stacks have a parallel orientation with respect to each other.

Molecular Modeling. In order to understand how the molecules are packed within these nanostructures, molecular modeling was performed on one-dimensional stacks (since 1D ribbon-like structures have been observed for **1** and **2** on mica and graphite substrates, respectively). Models for molecu-

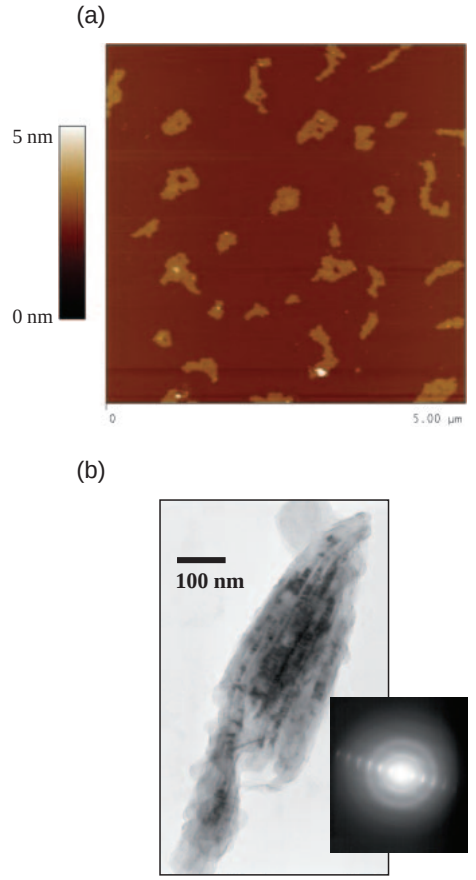

Fig. 7. (a) $5 \times 5\,\mu m^2$ AFM tapping-mode topographic image of **1** deposited from water on a mica substrate. (b) TEM micrograph of aggregates of **1** deposited from water on a carbon-coated microscope grid. Inset: selected area electron diffraction.

lar packing based on molecular mechanics (MM) and molecular dynamics (MD) simulations can shed light on the role of H-bonds in supramolecular organization. Figure 8 shows the most stable geometry for stacks of four molecules of **1** (a) and **2** (b). These models for cofacial stacks clearly indicate that:

(i) For both compounds, the oligothiophene segments have a strong tendency to be planar, parallel to each other. Between adjacent oligothiophenes, we observe a half-a-thiophene-unit displacement along their long axis. Note that this displacement along the long axis is also found for adjacent T6 molecules along the *c* direction of single crystals (low-temperature phase).[28]

(ii) For stacks of **2**, the oligo(ethylene oxide) segments nearly remain in the axis of the T6, in *trans–trans* or in *trans–gauche–trans* configuration. In contrast, in the case of **1**, there is a kink between the axis of the T6 segment and the $(EO)_5$ axis, due to the possibility to form hydrogen bonds between adjacent amide functions. This configuration allowing the formation of hydrogen bonds globally stabilizes the stacking (see below).

(iii) In terms of distance between the molecules, the spacing between adjacent T6 segments is homogeneous in the two systems; in the case of **1**, the distance between two adjacent T6 planes is 3.4–3.5 Å, while in the case of **2** it is slightly

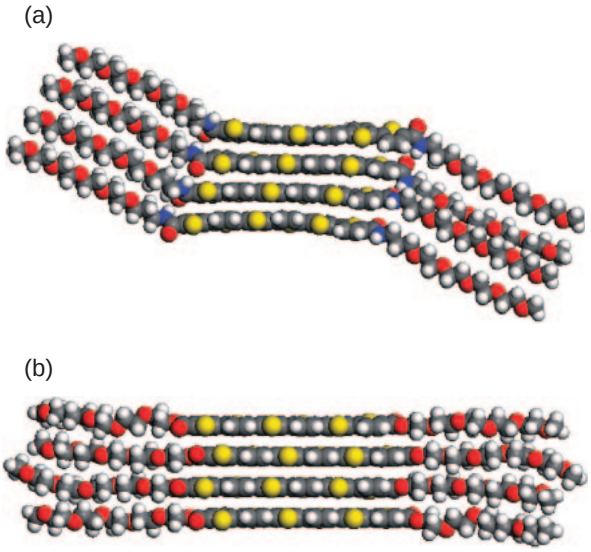

Fig. 8. Stable configurations of stacks of four molecules of (a) **1** and (b) **2**, shown with the plane of the oligothiophene segments perpendicular to the view. Sulfur atoms are yellow, nitrogen atoms blue, and oxygen atoms red.

Table 1. The Different Contributions to the Total Binding Energy per Molecule, in kcal mol^{-1}

Molecule	$E_{b,vdW}$	$E_{b,ES}$	$E_{b,H\text{-}bond}$	$\Delta E_{valence}$	$E_{b,tot}$
1	−35.6	−17.6	−3.7	+8.3	−48.6
2	−42.9	−1.8	0.0	+3.0	−41.7

larger (3.5–3.6 Å, i.e., a typical distance in parallel π-stacks of substituted oligo- and polythiophenes). Note that the value obtained for stacks of **1** agrees well with the *d*-spacing extracted from the electron-diffraction pattern. The slight difference in intermolecular distance between **1** and **2** is most likely due to the hydrogen bonds present in stacks of **1**.

In terms of stability, the binding energy per molecule is larger in stacks of **1** than in stacks of **2**, i.e. the stack is more "stable" in the case of **1**. Here, we define the mean binding energy per molecule as:

$$E_b = [E_{stack} - n^* E_{molecule}]/n, \quad (1)$$

where n is the number of molecules, E_{stack} is the energy of the stack and $E_{molecule}$ is the energy of the single molecule, in its most stable configuration. The total binding energies per molecule are −48.6 and −41.7 kcal mol^{-1} for **1** and **2**, respectively. Note that this difference of approximately 7 kcal mol^{-1} is rather large for systems that are similar in structure. To understand the origin of this difference, we calculate the binding energies for the different non-bonded contributions, i.e., van der Waals ($E_{b,vdW}$), electrostatic ($E_{b,ES}$), and H-bonds ($E_{b,H\text{-}bond}$), as well as the increase in valence energy when going from the single molecule to interacting molecules ($\Delta E_{valence}$), see Table 1. For stacks of **2**, we clearly find that the main origin of the interaction between molecules within the stack is the van der Waals interactions (note that a small change in valence energy means a small change in intramolecular geometry compared to the single molecule). For **1**, the situation is more complex: in

terms of van der Waals contribution and valence energy, the system is less stable compared to stacks of **2** (larger $E_{b,vdW}$ and $\Delta E_{valence}$), while the electrostatic and H-bond terms are lower (more stable), and lead to a more negative total binding energy in the stack for **1** compared to **2**. Note that, for stacks of **1**, the total H-bond stabilization is $-14.8\,kcal\,mol^{-1}$ for six H-bonds, i.e. $\approx -2.5\,kcal\,mol^{-1}$ per H-bond.

The nature of the molecular packing has a strong influence on the optical absorption spectra. In order to estimate the optical properties expected for the supramolecular organization obtained by theoretical modeling, we have computed the absorption spectrum of a single molecule as well as that of a stack of molecules extracted from the simulations and we have compared them to the corresponding experimental spectra measured in solution. The stack has been built by extracting the six central molecules from a stack optimized initially with ten molecules in order to avoid border effects; this size further ensures a good convergence of the calculated optical transition energies.[29] The INDO/SCI-calculated absorption spectrum shifts to the red by 0.54 eV when going from the isolated molecule to the stack; this value significantly overestimates the 0.30 eV shift observed experimentally. We attribute the significant difference between the calculated and experimental shifts to the fact that the torsion angles between adjacent thiophene rings is not actually close to zero for the isolated molecule, as predicted by the simulations both for the stack and for the isolated molecule. Accordingly, we have simulated in a second step the absorption spectrum of the isolated molecule with the torsion angle between adjacent rings set to a value of 30 degrees, as suggested by gas-phase quantum-chemical calculations.[30] In that case, the simulated and experimental spectral shifts are found to be in very nice agreement (0.27 and 0.30 eV, respectively), thus providing further support to the stacking models obtained in the simulations.

Induction of Chirality through Poly(glutamate) Complexation. Aggregates of **3** in aqueous medium were prepared by injecting small aliquots of a DMSO solution of the charged oligomer into water (see Experimental Section). UV–vis showed a structured absorption at 412 nm indicative of the formation of aggregates as a result of π–π stacking interactions. No CD effects were observed when these aggregates were prepared in the presence of enantiopure compounds such as *R*-camphorsulfonic acid (CSA) or L-aspartic acid. However, when the aggregates were prepared in the presence of poly(α-D-glutamate) (PDG, $M_w = 6400\,g\,mol^{-1}$), CD spectroscopy (Fig. 9) revealed a significant induced Cotton effect (ICD), similar to those detected for complexes of water soluble poly(thiophene)s with double-stranded DNA (dsDNA).[21] The bisignated, exciton coupled signal, with the positive lobe located around $\lambda = 440$ nm and the negative at approximately $\lambda = 390$ nm, was assigned to the π–π^* electronic transition in the sexithiophene chromophore. The positive lobe showed a vibronic progression, corresponding to the structure observed in the UV–vis spectrum, which displayed an absorption maximum at $\lambda_{max} = 412$ nm (Fig. 9).[31] The fluorescence spectrum of the complex displayed an emission band centered at $\lambda_{max} = 603$ nm, confirming the aggregation of the π-conjugated segments. The similarity in UV and fluorescence spectra of stacks of **3** with and without PDG does not allow speculation on differences in packing.

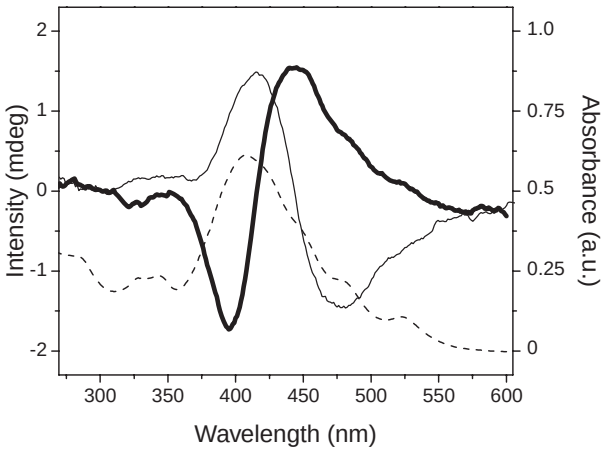

Fig. 9. CD (thick solid line) and normalized UV–vis (dashed line) spectra of aggregates of **3** formed in a solution of PDG ($M_w = 6400\,g\,mol^{-1}$) in water ([**3**] = $3.6\cdot10^{-5}$ M, [PDG] = $2.2\cdot10^{-6}$ M). Thin solid line: CD spectrum of **3** in the presence of PLG ($M_w = 5800\,g\,mol^{-1}$) in water, DMSO (2% v/v) ([**3**] = $3.6\cdot10^{-5}$ M, [PLG] = $2.2\cdot10^{-6}$ M).

We observed that the addition of a thousand-fold excess of Na^+ ions to the aggregates of **3**/PDG caused the disappearance of the CD signal. Also no CD signal was induced when, following an identical procedure, aggregates of the corresponding neutral analogue **1** were formed in the presence of PDG. From this we deduce that the charged end groups in **3** have an ion-exchange interaction with the PDG carboxylates inducing a conformational transition in the polypeptide from coil to α-helix, as described for complexes of polyglutamate and low molecular weight cationic amphiphiles.[32,33] Upon mixing **3** with poly(α-L-glutamate) (PLG) a CD signal of inversed sign but of equal intensity was obtained (Fig. 9). Moreover, aggregates prepared in the presence of DNA also showed a negative couplet in CD similar to the one observed for PLG, suggesting that the handedness of the template is reflected in the helical organization of the sexithiophene segments. DNA and PLG, both forming a P-helix,[34] gave indeed rise to an ICD couplet that can be assigned to a left-handed helical organization of the sexithiophene segments.[35] Importantly, no ICD signal was observed when a solution of PDG in water was added to pre-formed assemblies of **3**. The ICD of **3**/PDG mixtures disappeared upon standing for one day at room temperature. Regarding the mechanism of formation we propose that the polypeptide acts as a chiral template, directing the formation of the assembly such that a helical bias is induced in the aggregate. This apparently meta-stable state eventually is lost, and the aggregated oligomers may be released from the template to find a more stable configuration, presumably the one that is formed in the absence of PDG. Therefore, we have to conclude that for achiral sexithiophenes, a non-chiral supramolecular packing is favored, only steric constraints by either stereocenters in the side-chains[4] or chiral complexing agents, like PDG, can tilt the supramolecular packing into a helical stack.

With the aim to obtain insight into this templating process, we determined the COO^-/NH_3^+ ratio for which the maximum

Table 2. The Anisotropy Factor $g_{abs} = \Delta\varepsilon/\varepsilon$ as a Function of the Ratio between the Glutamate Residues and **3**[a)]

[**3**] /M	[PDG] /M	COO^-/NH_3^+	g_{abs} (392 nm)
$3.6\cdot10^{-5}$	$3.5\cdot10^{-5}$	20.9	0.0
$3.6\cdot10^{-5}$	$3.5\cdot10^{-6}$	2.1	$-2.0\cdot10^{-4}$
$3.6\cdot10^{-5}$	$2.2\cdot10^{-6}$	1.4	$-2.1\cdot10^{-4}$
$3.6\cdot10^{-5}$	$9.5\cdot10^{-7}$	0.6	$-1.6\cdot10^{-4}$
$3.6\cdot10^{-5}$	$5.6\cdot10^{-7}$	0.4	$-9.6\cdot10^{-5}$

a) M_w (PDG) = 6400 g mol^{-1}.

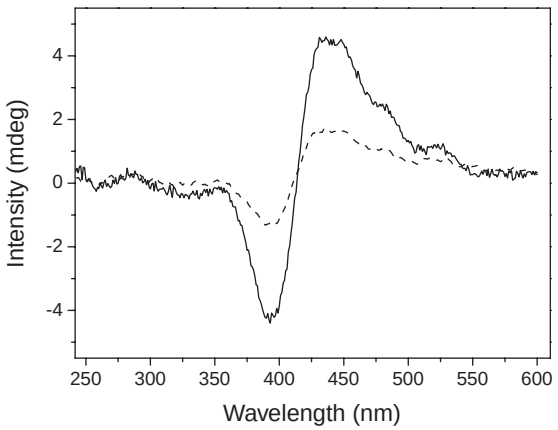

Fig. 10. CD spectrum of **3** in the presence of PDG with $M_w = 6400\,g\,mol^{-1}$ (solid line) and PDG with $M_w = 44700\,g\,mol^{-1}$ (dashed line). [**3**] = $3.6\cdot10^{-5}$ M in water, DMSO (2% v/v). [PDG] = $2.2\cdot10^{-6}$ M.

CD effect was found to be approximately 1.5 (Table 2). It was also observed that at this ratio the magnitude of the ICD couplet decreased to approximately 30% when the molecular weight of the PDG was increased from 6400 to 44700 g mol^{-1}, (Fig. 10) similar to what was reported for the complexation of PDG with low molecular weight cationic surfactants.[32b] This agrees well with a kinetic process in which the chirality of the template is temporarily transferred to the stacks of **3**. In addition, CD spectra of mixed assemblies of **1** and **3**, formed in the presence of PDG were recorded and their maximum intensities were plotted as function of the molar fraction of the actively interacting component (**3**) in the heterogeneous stack (Fig. 11). The observed non-linear behavior suggests that the two oligomers are effectively mixed in the stacks and that the dilution of interacting points as determined by the presence of **1** can tune the supramolecular chirality by specific electrostatic interaction.

Conclusion

We have demonstrated that the introduction of amide functionalities as linkers between the oligo(ethylene oxide) chains and the sexithiophene core of the amphiphilic oligomer **1** affects its aggregation behavior. It was shown that **1** has a higher tendency to aggregate in solvents in which the ester derivative **2** is molecularly dissolved. The aggregates observed showed morphologies that ranged from flat irregular platelets to well-defined rods, suggesting that these are formed as a

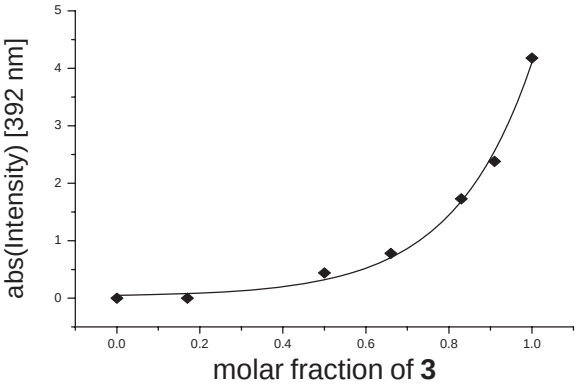

Fig. 11. Dependence of the CD intensity (absolute value) on the molar fraction of **3** in mixtures of **1** and **3**, in the presence of PDG ($M_w = 6400\,g\,mol^{-1}$). Note that the curve is drawn as guide to the eye.

result of a delicate interplay of solvent and surface interactions in conjunction with hydrogen-bonding and π–π interactions. UV–vis and fluorescence spectra of solutions showed that the aggregated state is predominant in protic solvents such as *n*-butanol and water. The effect of the hydrogen bonds on the stability of the aggregates in protic solvent was demonstrated by variable-temperature experiments in *n*-butanol revealing a 20 °C higher transition from the aggregated to the molecularly dissolved state as compared to the corresponding ester derivative **2**. In water, a further red shift of the π–π transition was observed compared to the ester and the aggregates did not show a transition to the molecularly dissolved state even up to temperatures as high as 90 °C. Transmission electron microscopy in combination with selected area electron diffraction showed that these aggregates consisted of parallel oriented stacks of **1** with a π–π distance of 3.5 Å. The simulations show the similarities in terms of morphology of one-dimensional stacks of **1** or **2**. In the case of **2**, the type of ordering is mainly due to the π-stacking of the conjugated segments. Even though the π-stacking also occurs in assemblies of **1**, it is important to notice that strong stabilization of stacks of **1** compared to stacks of **2** is brought by the H-bonds, These interactions position the molecules of **1** at slightly smaller distances compared to stacks of **2**. Note that these results fully support the spectroscopic results, and bring a clear picture in terms of structural and energetic information on the differences between stacks of **1** and **2**. From these results it is clear that the introduction of amide functionalities at the periphery of a linear aromatic core causes the generation of ordered stacks of molecules most likely aided by the formation of hydrogen bonds that stabilize the π–π interactions. This is a tool that can allow further control over the molecular organization of this class of π-conjugated materials.

The introduction of a terminal ammonium group in the oligo(ethylene oxide) chains of **3** significantly adds to the functionality of the oligomeric stacks. Moreover, the induction of chirality through complexation of polyanionic (bio)macromolecules forms a new concept in the organization of π-conjugated oligomers. Although the molecular details of the templating process still need to be resolved, we believe that this new approach can be extended beyond the examples pre-

sented here and that it holds great promise for the organization of π-conjugated segments in dynamic supramolecular materials. These water-soluble conjugated polymers present therefore potential use as a new class of high-sensitive rapid-response chemical and biological sensors.[36] The fluorescence of these polymers is sensitive to very small amount of charged molecules that quench the excited state by energy transfer or electron transfer.[37] This phenomenon may be exploited for biosensing by coupling a quencher to a biological ligand.

Experimental

General Methods. NMR spectra were recorded on a Varian Mercury Vx at frequencies of 400 and 100 MHz for ^{1}H and ^{13}C nuclei or a Varian Gemini 2000 at frequencies of 300 and 75 MHz for ^{1}H and ^{13}C nuclei, respectively. Signals are reported as singlet (s), doublet (d), double doublet (dd), triplet (t), quartet (q), quintet (quint), and multiplet (m). Matrix-assisted laser desorption ionization time-of-flight mass spectrometry (MALDI-TOF MS) was performed on a Perseptive DE PRO Voyager MALDI-TOF mass spectrometer using a dithranol matrix. UV/visible absorption spectra were recorded on a Perkin-Elmer Lambda 900 spectrophotometer. Fluorescence spectra were recorded on an Edinburgh Instruments FS920 double-monochromator spectrometer and a Peltier-cooled red-sensitive photomultiplier. For temperature-dependent (−10–90 °C) solution measurements the spectrophotometers were equipped with a thermostated sample holder controlled by a water-ethylene glycol bath. Spectra are recorded after a period of one hour in order to let the system stabilize to the desired temperature. Transmission electron microscopy was carried out using a JEOL JEM (2000-FX) operating at 120 kV; a droplet of solution was placed on a Cu-grid (200 mesh, C covered, for TEM), and allowed to dry for a few seconds, after which the excess fluid was removed by blotting.

Atomic Force Microscopy (AFM). AFM measurements were performed under ambient conditions using a Digital Instrument Multimode Nanoscope IV operating in the tapping-mode regime. Microfabricated silicon cantilever tips (NSG01 or NSG11) with a resonance frequency of approximately 150 kHz and a spring constant of about 5.5 Nm^{-1} were used. Aggregates of **1** in water were deposited on mica following the same procedure used for the TEM sample, while chloroform and toluene solutions of **1** were slowly evaporated on the mica substrate in a solvent-saturated atmosphere. The measured width of the features was corrected for a broadening effect, which is related to the radius of the tip apex. By using a simple model based on a spherical tip apex (with radius R) and a rectangular cross-section of the ribbon (of height h), the broadening d is given by $2\sqrt{(2R-h)\cdot h}$.[38] Solutions of **1** in toluene, THF, or *n*-butanol were prepared by sonication. A typical procedure for the preparation of aggregates of **1** in water is the following: 50 μL of a THF solution of **1** ($1.8\cdot10^{-3}$ M) were injected in 2.5 mL of water, THF was then removed by extensive purging with nitrogen gas.

Molecular Modeling. For the molecular modeling calculations, the stable conformations of the molecules were found by conformer search using the DREIDING 2.21 force field,[39] which has been previously tested for comparable systems.[40] Note that the atom charges were assigned using the PCFF force field, which correctly ascribes the charges in organic molecules. The energy minima parameters were found using the Conjugate Gradient algorithm, with the following convergence criteria: RMS Force: 10^{-3} kcal mol^{-1} $Å^{-1}$; Energy difference: 10^{-5} kcal mol^{-1}; RMS displacement: 3.10^{-5} Å. Stacks of four molecules were built in which adjacent sexithiophenes were in full cofacial configuration, at a distance of 3.7 Å to each other. A Molecular Mechanics (MM) simulation was first carried out, in order to start from a relatively stable configuration; this led to a slight displacement of adjacent oligothiophenes along the molecular axis and along their stacking axis. A Molecular Dynamics (MD) run at 300 K was then performed using the canonical ensemble (constant N, V, T) with the Hoover thermostat. Simulations were performed using the "Verlet-leapfrog" algorithm with a relaxation time of 0.1, with a time step of 1 femtosecond. The simulation duration was set to 500 picoseconds (with snapshots of the trajectory recorded every 50 fs). The most stable structures (potential energy minima) were then extracted and are submitted to a final Molecular Mechanics minimization; the global minimum was defined as the lowest potential energy. For all the simulations steps (MM and MD), the DREIDING 2.21 force field was used; the non-bonded interactions were described using the Spline method with cut-on and cut-off parameters set to 11.0 and 14.0 Å, respectively for the van der Waals and Coulomb terms, and to 4.0 and 4.5 Å, respectively for Hydrogen-bonds terms. Note that the stable configuration found for the four-molecules stacks is maintained when the system is extended to a ten-molecules stack. On the basis of the molecular geometries obtained by modeling, the absorption spectra have been simulated with the help of the semiempirical Hartree–Fock Intermediate Neglect of Differential Overlap (INDO) Hamiltonian (as parameterized by Zerner and co-workers[41]) coupled to a configuration interaction scheme involving only single excitations (SCI). Since the lowest optical transitions mostly originate from electronic excitations between the frontier π-electronic levels, the configurations have been generated here by promoting one electron from one of the highest ten occupied molecular orbitals to one of the lowest ten unoccupied. The long saturated chains do not participate to the description of the frontier electronic levels and have thus been replaced by methyl-amide groups when simulating the optical absorption spectra.

Materials General. 5′-Bromo-2,2′-bithiophene-5-carbonyl chloride (**6**)[4] and 5,5′-bis(trimethylstannyl)-2,2′-bithiophene (**8**)[42] were prepared as reported elsewhere. (1*R*)-(−)-Camphorsulfonic acid ammonium salt (CSA), L-aspartic acid monopotassium salt hydrate (Asp), poly(α-D-glutamic acid) sodium salt (PDG, M_w = 6400 g mol^{-1} and 44700 g mol^{-1}, PDI = 1.3), poly(α-L-glutamic acid) sodium salt (PLG, M_w = 5800 g mol^{-1}, PDI = 1.2) and dsDNA from salmon sperm ($M_w \approx 10^6$ g mol^{-1}) were obtained from Sigma. Water was purified by means of a Barnstead EASYpure LF system. DMA was distilled from BaO, THF from Na/K, and dichloromethane from P_2O_5. All other solvents and reagents were commercial products and were used as received.

4,7,10,13,16-Pentaoxaheptadecanenitrile (4). A solution of 5.53 g (26.70 mmol) of tetra(ethylene glycol) mono methyl ether in acrylonitrile (19.32 g) was cooled in an ice bath, after which 14.1 mg (0.251 mmol) of pulverized KOH was added and vigorously stirred. After 1.5 h the reaction was quenched by addition of a few drops of concentrated HCl. Acrylonitrile was evaporated in vacuo and a yellow oil/solid mixture was obtained. The mixture was then redissolved in CH_2Cl_2, and filtrated on a glass filter in order to remove the solid (polyacrylonitrile). The solvent was then evaporated in vacuo. The title product **4** (6.76 g, 99.3%) was obtained as pale yellow oil and used without further purification. ^{1}H NMR (400 MHz, $CDCl_3$): δ 3.72 (t, J = 6.6 Hz, 2H, OCH_2CH_2CN), 3.67–3.62 (m, 14H, CH_2O), 3.55–3.53 (m, CH_2-OCH_3), 3.37 (s, 3H, CH_3O), 2.62 (t, J = 6.6 Hz, 2H, CH_2CN).

^{13}C NMR (75 MHz, $CDCl_3$): δ 117.72, 71.68, 70.49, 70.42, 70.36, 70.32, 70.26, 65.70, 58.76, 18.62. MS (MALDI-TOF) m/z 284.22 (calcd. $[M + Na]^+$ 284.15).

4,7,10,13,16-Pentaoxaheptadecylamine (5). To a solution of **4** (4.00 g, 15.30 mmol) in 20 mL of THF, 63 mL of a 1.0 M solution of $BH_3 \cdot$THF were added dropwise. The mixture was refluxed for 3.5 h. After cooling to room temperature, the reaction was quenched by slow addition of 35 mL of methanol and 4 mL of concentrated HCl. The solvent was evaporated in vacuo. The residue was dissolved in 40 mL aqueous NaOH (2 M) and extracted with CH_2Cl_2 (15 × 25 mL). The organic layers were collected and dried over Na_2SO_4. After solvent evaporation in vacuo, the pure product **5** (3.94 g, 97%) was obtained as colorless oil, which was stored under argon and protected from light. ^{1}H NMR (400 MHz, $CDCl_3$): δ 3.67–3.55 (m, 18H, CH_2O), 3.34 (s, 3H, CH_3O), 2.89 (m, 2H, OCH$_2$CH$_2$CH_2NH$_2$), 1.85 (ps q, $J = 6.0$ Hz, 2H, OCH$_2$CH_2CH$_2$NH$_2$). ^{13}C NMR (100 MHz, $CDCl_3$): δ 71.67, 70.50, 70.46, 70.41, 70.38, 70.31, 70.23, 70.20, 70.09, 58.90, 39.61, 30.68. MS (MALDI-TOF) m/z 266.37 (calcd. $[M + H]^+$ 266.20).

5′-Bromo-2,2′-bithiophenyl-5-carboxylic Acid (4,7,10,13,16-Pentaoxaheptadecyl)amide (7). A solution of **6**[4] (0.540 g, 1.755 mmol) in diethyl ether (120 mL) was added dropwise over one hour to an ice-cooled suspension of **5** (0.465 g, 1.752 mmol) in diethyl ether (20 mL) containing triethylamine (0.186 g, 1.838 mmol). After the addition, the reaction was allowed to reach room temperature and was stirred overnight. After filtration through a glass filter, the solvent was removed in vacuo and a pale yellow solid was obtained, which was purified by column chromatography (silica, CH_2Cl_2 followed by methanol/CH_2Cl_2, 1:9 v/v) and reprecipitated from hexane to yield pure **7** as a white powder (0.752 g, 80%). Mp 72–73 °C; ^{1}H NMR (400 MHz, $CDCl_3$): δ 7.40 (d, 1H, $J = 3.6$ Hz), 7.11 (br, 1H, N*H*CO), 7.03 (d, 2H, $J = 3.6$ Hz), 6.98 (m, 2H), 3.69–3.50 (m, 20H, CH_2O), 3.34 (s, 3H, CH_3O), 1.89 (ps q, 2H, $J = 6.0$ Hz, OCH$_2$CH_2CH$_2$NHCO). ^{13}C NMR (100 MHz, $CDCl_3$): δ 161.10, 140.13, 138.90, 137.98, 130.71, 128.09, 124.68, 123.90, 112.09, 71.90, 70.84, 70.57, 70.51, 70.42, 70.38, 70.24, 59.04, 39.22, 28.73. MS (MALDI-TOF) m/z 560.09 (calcd. $[M + Na]^+$ 560.06). Anal. Calcd for $C_{21}H_{30}BrNO_6S_2$: C, 47.01; H, 5.64; N, 2.61%. Found: C, 47.26; H, 5.36; N, 2.62%.

2,2′;5′,2″;5″,2‴;5‴,2⁗;5⁗,2⁗′-Sexithiophene-5,5⁗′-dicarboxylic Acid Bis[(4,7,10,13,16-pentaoxaheptadecyl)amide] (1). Under inert atmosphere, 291.0 mg (0.542 mmol) of **7**, 134.6 mg (0.274 mmol) of **8**, and 31.6 mg (0.027 mmol) of $Pd(PPh_3)_4$ were dissolved in dry DMA (2.5 mL). After three freeze–pump–thaw cycles, the mixture was heated to 120 °C and stirred for 21 h. After cooling to room temperature, chloroform (100 mL) was added to the mixture and the resulting red solution was filtered through a short plug of celite™. The solvent was removed in vacuo and the obtained residue was precipitated in *n*-hexane. The resulting suspension was centrifuged to collect a solid, which was further washed with cold water in order to remove any residual tin derivative. The crude product was purified twice by column chromatography (preparative SEC, CH_2Cl_2) to give **1** as a red solid (143 mg, 49%). Mp 310–322 °C (decomp.); ^{1}H NMR (400 MHz, $CDCl_3$): δ 7.44 (d, 2H, $J = 3.6$ Hz), 7.24 (br, 2H, N*H*CO), 7.16 (d, 2H, $J = 3.6$ Hz), 7.10 (m, 8H), 3.71–3.50 (m, 40H, CH_2O, CH_2NHCO), 3.35 (s, 6H, CH_3O), 1.90 (ps q, $J = 6.0$ Hz, 4H, OCH$_2$CH_2CH$_2$-NHCO). ^{13}C NMR (100 MHz, $CDCl_3$): δ 161.44, 140.99, 138.10, 136.88, 136.16, 135.82, 135.61, 128.39, 125.49, 124.72, 124.55, 124.53, 123.80, 71.87, 70.71, 70.55, 70.51, 70.48, 70.43, 70.39, 70.23, 59.00, 38.99, 28.64. IR: ν 3340, 3060, 2865, 1626, 1539, 1219, 1097, 788. MS (MALDI-TOF) m/z 1075.88 (calcd. $[M]^+$ 1076.28). Anal. Calcd for $C_{50}H_{64}N_2O_{12}S_6$: C, 55.74; H, 5.99; N, 2.60%. Found: C, 53.97; H, 5.40; N, 2.72%.

4,7,10,13,16-Pentaoxanonadecane-1,14-dinitrile (9). A solution of 9.99 g (51.43 mmol) of tetraethylene glycol in 38.60 g (727.48 mmol) of acrylonitrile was cooled in an ice bath, after which 29.0 mg (0.517 mmol) of pulverized KOH was added and the solution was vigorously stirred. After 1.5 h, the reaction was quenched by addition of a few drops of concentrated HCl. Acrylonitrile was evaporated in vacuo and a yellow oil/solid mixture was obtained. The mixture was then redissolved in CH_2Cl_2, and filtred on a glass filter in order to remove the solid (polyacrylonitrile). The solvent was then evaporated in vacuo. The title product **9** (15.30 g, 99%) was obtained as a pale yellow oil and used without further purification. ^{1}H NMR (300 MHz, $CDCl_3$): δ 3.65 (t, $J = 6.3$ Hz, 4H, OCH_2CH$_2$CN), 3.60–3.56 (br, 16H, CH_2O), 2.58 (t, $J = 6.3$ Hz, 4H, CH_2CN). ^{13}C NMR (75 MHz, $CDCl_3$): δ 117.76 (s, *C*N), 70.39, 70.35, 70.24, 70.20, 65.61 (s, O*C*H$_2$CH$_2$-CN), 18.57 (s, *C*H$_2$CN). MS (MALDI-TOF) m/z 323.25 (calcd. $[M + Na]^+$ 323.16).

4,7,10,13,16-Pentaoxanonadecane-1,19-diamine (10). To a solution of **9** (4.00 g, 13.31 mmol) in 20 mL of THF, 109 mL of a 1.0 M solution of $BH_3 \cdot$THF were added dropwise. The mixture was refluxed for 3.5 h. After cooling to room temperature, the reaction was quenched by slow addition of 30 mL of methanol and 7 mL of concentrated HCl. The solvent was evaporated in vacuo. The residue was dissolved in 50 mL of NaOH (2.0 M) and extracted with CH_2Cl_2 (15 × 25 mL). The organic layers were collected and dried over Na_2SO_4. After solvent evaporation **10** was obtained as a colourless oil (4.02 g, 98%), which was stored under argon and protected from light. ^{1}H NMR (400 MHz, $CDCl_3$): δ 3.62–3.51 (20H, CH_2O), 2.78 (t, $J = 6.6$ Hz, 4H, NH$_2$CH_2CH$_2$CH$_2$O), 1.86 (s, 4H, NH_2CH$_2$CH$_2$CH$_2$O), 1.71 (ps quint, $J = 6.6$ Hz, 4H, NH$_2$CH$_2$CH_2CH$_2$O). ^{13}C NMR (100 MHz, $CDCl_3$): δ 70.40, 69.96 (s, NH$_2$CH$_2$CH$_2$CH$_2$O*C*H$_2$), 69.29 (s, NH$_2$CH$_2$CH$_2$*C*H$_2$O), 39.43 (s, NH$_2$*C*H$_2$CH$_2$CH$_2$O), 32.98 (s, NH$_2$CH$_2$*C*H$_2$CH$_2$O). MS (MALDI-TOF) m/z 309.24 (calcd. $[M + H]^+$ 309.24).

19-(*tert*-Butoxycarbonylamino)-4,7,10,13,16-pentaoxanonadecylamine (11). To a dioxane solution (10 mL) of **10** (2.854 g, 9.254 mmol), kept under vigorous stirring at room temperature, a dioxane solution (10 mL) of di-*t*-butyl dicarbonate (348.0 mg, 1.594 mmol) was added dropwise over a period of 3 h. The mixture was stirred for an additional 20 h. The solvent was then removed in vacuo, the residue dissolved in water (25 mL) and rinsed with CH_2Cl_2 (5 × 50 mL). The combined organic layers were rinsed with brine (4 × 50 mL) and concentrated under reduced pressure. The obtained oil was dissolved in CH_2Cl_2 (20 mL) and washed with water (4 × 10 mL). The organic solution was dried over $MgSO_4$ and after solvent evaporation in vacuo, pure **11** (440 mg, 68%) was obtained as a pale yellow oil, which was stored under argon and protected from light. ^{1}H NMR (400 MHz, $CDCl_3$): δ 5.04 (br, 1H, N*H*CO), 3.67–3.51 (m, 20H, CH_2O), 3.21 (m, 2H, CH_2NHCO), 2.78 (t, $J = 6.6$ Hz, 2H, CH_2-NH$_2$), 1.71–1.68 (m, 4H, NH$_2$CH$_2$CH_2CH$_2$O, CONHCH$_2$CH_2-CH$_2$O), 1.42 (s, 9H, (CH_3)$_3$C). ^{13}C NMR (100 MHz, $CDCl_3$): δ 156.00, 70.58, 70.56, 70.53, 70.19, 70.14, 69.56, 69.41, 39.58, 38.52, 33.38, 29.59, 28.42. MS (MALDI-TOF) m/z 409.26 (calcd. $[M + H]^+$ 409.29).

5′-Bromo-2,2′-bithiophenyl-5-carboxylic Acid [19-(*tert*-Butoxycarbonylamino)-4,7,10,13,16-pentaoxanonadecyl]amide (12). A solution of 5-bromo-2,2′-bithiophene-5′-carbonyl chloride[4b]

(**6**) (0.293 g, 0.952 mmol) in diethyl ether (100 mL) was added dropwise over one hour to a cooled (ice-bath) suspension of **11** (0.388 g, 0.950 mmol) in diethyl ether (10 mL) containing triethylamine (0.106 g, 1.047 mol). The reaction was then allowed to reach room temperature and was kept under stirring overnight. After filtration through a glass filter, the solvent was removed in vacuo. The crude product was purified by column chromatography (silica, CH_2Cl_2 followed by methanol/CH_2Cl_2, 1:9) to give pure **12** as a pale yellow oil (0.350 g, 54%). ^{1}H NMR (400 MHz, $CDCl_3$): δ 7.41 (d, 1H, $J = 3.6$ Hz), 7.18 (br, 1H, N*H*CO), 7.03 (d, 2H, $J = 3.6$ Hz), 6.98 (m, 2H), 4.98 (br, 1H, N*H*COOC-$(CH_3)_3$), 3.68–3.49 (m, 22H, C*H*$_2$O, C*H*$_2$NHCO), 3.21 (m, 2H, C*H*$_2$NHCO$(CH_3)_3$), 1.88 (ps quint, $J = 6.0$ Hz, 2H, CONHCH$_2$-C*H*$_2$CH$_2$O), 1.73 (ps quint, $J = 6.0$ Hz, 2H, $(CH_3)_3$CONHCH$_2$-C*H*$_2$CH$_2$O), 1.43 (s, 9H, $(CH_3)_3$C). ^{13}C NMR (100 MHz, $CDCl_3$): δ 161.33, 156.03, 140.27, 138.47, 138.14, 130.84, 124.79, 124.00, 112.78, 70.66, 70.58, 70.54, 70.47, 70.40, 70.37, 70.19, 70.14, 69.21, 38.95, 38.51, 29.61, 28.63, 28.44. MS (MALDI-TOF) m/z 703.15 (calcd. $[M + Na]^+$ 703.15).

2,2′;5′,2″;5″,2‴;5‴,2⁗;5⁗,2⁗′;5⁗′,2⁗″-Sexithiophene-5,5⁗′-dicarboxylic Acid Bis[(19-(*tert*-butoxycarbonylamino)-4,7,10,13,16-pentaoxanonadecyl))amide] (13). Under an inert atmosphere, 316.6 mg (0.466 mmol) of **12**, 115.7 mg (0.235 mmol) of 5,5′-bistrimethylstannyl-2,2′-bithiophene (**8**) and 27.0 mg (0.023 mmol) of $Pd(PPh_3)_4$ were dissolved in dry DMA (2.0 mL). After three freeze–pump–thaw cycles, the mixture was heated to 120 °C and stirred for 21 h. After cooling to room temperature, chloroform (100 mL) was added to the mixture and the resulting red solution was filtered through a short plug of celite™. The solvent was removed in vacuo and the obtained residue was precipitated in *n*-hexane. The resulting suspension was centrifuged to collect a solid, which was further washed with cold water in order to remove any residual tin derivative. The crude product was purified twice by column chromatography (preparative SEC, CH_2Cl_2) to give **13** as a red solid (159 mg, 50%). Decomp. 230 °C; ^{1}H NMR (400 MHz, $CDCl_3$): δ 7.44 (d, 2H, $J = 3.6$ Hz), 7.22 (br, 2H, N*H*CO), 7.15 (d, 2H, $J = 3.6$ Hz), 7.10 (m, 8H), 5.00 (br, 2H, N*H*COOC$(CH_3)_3$), 3.69–3.48 (m, 44H, C*H*$_2$O, C*H*$_2$NHCO), 3.18 (m, 4H, C*H*$_2$NHCO$(CH_3)_3$), 1.9 (ps quint, $J = 6.0$ Hz, 4H, CONHCH$_2$C*H*$_2$CH$_2$O), 1.73 (ps quint, $J = 6.0$ Hz, 4H, $(CH_3)_3$-CONHCH$_2$C*H*$_2$CH$_2$O), 1.43 (s, 18H, $(CH_3)_3$C). ^{13}C NMR (100 MHz, $CDCl_3$): δ 161.42, 156.01, 140.95, 138.08, 136.83, 136.10, 135.76, 135.56, 128.40, 125.45, 124.69, 124.52, 124.49, 123.77, 70.57, 70.52, 70.49, 70.40, 70.36, 70.18, 70.12, 69.51, 38.89, 38.50, 29.59, 28.69, 28.43. IR: ν 3343, 3067, 2866, 1693, 1627, 1538, 1259, 1095, 790. MS (MALDI-TOF) m/z 1385.36 (calcd. $[M + Na]^+$ 1385.46).

***N*,*N*′-Bis(19-ammonium-4,7,10,13,16-pentaoxanonadecyl)-2,2′;5′,2″;5″,2‴;5‴,2⁗;5⁗,2⁗′;5⁗′,2⁗″-sexithiophene-5,5⁗′-dicarboxamide Bis(trifluoroacetate) (3).** To a solution of **13** (100.0 mg, 0.073 mmol) in 9.0 mL of CH_2Cl_2, 1.0 mL of TFA was added dropwise over a few minutes at room temperature. The mixture was stirred overnight and then concentrated in vacuo. The orange residue was suspended in 10 mL of benzene, and the solvent was again evaporated under reduced pressure in order to remove the excess TFA. The resulting diamine salt (103 mg, 100%) was used without further purification. ^{1}H NMR (400 MHz, d_6-DMSO): δ 8.56 (br, NH_3^+), 7.72 (d, 2H, $J = 3.6$ Hz), 7.6 (br, 2H, N*H*CO), 7.44 (d, 2H, $J = 3.6$ Hz), 7.39 (m, 8H), 3.62–3.25 (m, 48H, C*H*$_2$O, C*H*$_2$NHCO, C*H*$_2$NH$_3^+$), 1.77 (m, 8H, CONHCH$_2$C*H*$_2$CH$_2$O, NH$_2$CH$_2$C*H*$_2$CH$_2$O). IR: ν 3339, 3062, 2923, 1678, 1629, 1540, 1204, 1127, 790. MS (MALDI-TOF) m/z 1163.32 (calcd. $[(M - 2TFAH) + H]^+$ 1163.36), 1185.30 (calcd. $[(M - 2TFAH) + Na]^+$ 1185.36).

Preparation of the PDG Solutions. A typical procedure for the preparation of an aqueous solution of **3** is the following: 50 μL of a DMSO solution of **3** ($1.8 \cdot 10^{-3}$ M) were injected in 2.5 mL of water. For the preparation of optically active **3**/PDG mixtures: 50 μL of a DMSO solution of **3** ($1.8 \cdot 10^{-3}$ M) were injected in 2.5 mL of water containing PDG ($2.25 \cdot 10^{-6}$ M). The final concentration of **3** was $3.6 \cdot 10^{-5}$ M. The same procedure was adopted for PDG of different molecular weights or for PLG. Mixtures of **3** with CSA or Asp were prepared either adding a concentrated solution of CSA or Asp in water to an aqueous solution of **3** or injecting 50 μL of a DMSO solution of **3** in 2.5 mL of water containing CSA or Asp. In both cases the final concentration of **3** was $3.6 \cdot 10^{-5}$ M, while the concentrations of CSA or Asp varied between $6 \cdot 10^{-4}$ and $6 \cdot 10^{-2}$ M. The CD spectrum was recorded a few minutes after mixing. The preparation of mixture containing NaCl was performed adding the salt directly to the **3**/PDG aqueous solution (final concentration of NaCl: 0.1 M). For the preparation of mixed aggregates of **2** and **3**, two solutions of identical concentration in DMSO ($1.8 \cdot 10^{-3}$ M) of the two compounds were mixed in different proportion. Prior to injecting the resulting DMSO solution in water containing PDG ($M_w = 6400$ g mol^{-1}), the mixture of **2** and **3** was heated with a heat gun (≈80 °C) and cooled again at room temperature. The procedure adopted for the preparation of **3**/dsDNA optically active mixtures is the same described for **3**/PDG mixtures, with [dsDNA] ≈ $4 \cdot 10^{-8}$ M.

The authors thank W. James Feast (University of Durham, U.K.) and Oliver Henze (Elastogran Gmbh, Lemförde, Germany) for fruitful discussion. The collaboration between Mons and Eindhoven has been conducted within the European Commission Training and Mobility of Researchers Network LAMINATE (Large Area Molecular electronics Involving a Novel Approach to Training and Education—Contract Number HPRN-CT-2000-00135). Research in Mons has been conducted within the framework of the Belgian Science Policy Interuniversity Attraction Poles Program (PAI V/3). Research in Mons is also supported by the European Commission, the Government of the Région Wallonne (Phasing Out-Hainaut) and the Belgian National Fund for Scientific Research FNRS/FRFC. M.S. and V.L. acknowledge the F.R.I.A. (Belgium) for a doctoral scholarship. Ph. L. is chercheur quali fié du FNRS (Belgium).

References

1 a) *Electronic Materials: The Oligomer Approach*, ed. by K. Müllen, G. Wegner, Wiley-VCH, Weinheim, Germany, **1998**. b) D. Fichou, *J. Mater. Chem.* **2000**, *10*, 571. c) F. Garnier, G. Horowitz, X. Peng, D. Fichou, *Adv. Mater.* **1990**, *2*, 592. d) G. Horowitz, D. Fichou, X. Peng, Z. Xu, F. Garnier, *Solid State Commun.* **1989**, *72*, 381. e) F. J. M. Hoeben, P. Jonkheijm, E. W. Meijer, A. P. H. J. Schenning, *Chem. Rev.* **2005**, *105*, 1491. f) M. R. Wasielewski, *J. Org. Chem.* **2006**, *71*, 5051. g) J. A. A. W. Elemans, R. van Hameren, R. J. M. Nolte, A. E. Rowan, *Adv. Mater.* **2006**, *18*, 1251.

2 a) H. E. Katz, J. G. Laquindanum, A. J. Lovinger, *Chem. Mater.* **1998**, *10*, 633. b) H. E. Katz, *J. Mater. Chem.* **1997**, *7*, 369. c) H. E. Katz, A. Dodabalapur, L. Torsi, D. Elder, *Chem. Mater.* **1995**, *7*, 2238. d) J. P. Parakka, M. P. Cava, *Tetrahedron*

1995, *51*, 2229. e) F. Garnier, A. Yassar, R. Hajlaoui, G. Horowitz, F. Deloffre, B. Servet, S. Ries, P. Alnot, *J. Am. Chem. Soc.* **1993**, *115*, 8716. f) A. R. Murphy, P. C. Chang, P. VanDyke, J. Liu, J. M. J. Fréchet, V. Subramanian, D. M. DeLongchamp, S. Sambasivan, D. A. Fisher, E. K. Lin, *Chem. Mater.* **2005**, *17*, 6033. g) A. Dell'Aquila, P. Mastrorilli, C. F. Nobile, G. Romanazzi, G. P. Suranna, L. Torsi, M. C. Tanese, D. Acierno, E. Amendola, P. Morales, *J. Mater. Chem.* **2006**, *16*, 1183. h) G. Zotti, S. Zecchin, B. Vercelli, M. Pasini, S. Destri, F. Bertini, A. Berlin, *Chem. Mater.* **2006**, *18*, 3151.

3 a) F. Brustolin, F. Goldoni, E. W. Meijer, N. A. J. M. Sommerdijk, *Macromolecules* **2002**, *35*, 1054. b) T. Bjørnholm, D. R. Greve, N. Reitzel, T. Hassnkam, K. Kjaer, P. B. Howes, N. B. Larsen, J. Bøgelund, M. Jayaraman, P. C. Ewbank, R. D. McCullough, *J. Am. Chem. Soc.* **1998**, *120*, 7643. c) L. Belobrzeckaja, G. Bajo, A. Bolognesi, M. Catellani, *Synth. Met.* **1997**, *84*, 195. d) R. D. McCullough, S. P. Williams, *Chem. Mater.* **1995**, *7*, 2001. e) I. Lévesque, M. Leclerc, *J. Chem. Soc., Chem. Commun.* **1995**, 2293. f) I. Lévesque, M. Leclerc, *Chem. Mater.* **1996**, *8*, 2843. g) R. D. McCullough, S. P. Williams, *J. Am. Chem. Soc.* **1993**, *115*, 11608. h) J. H. Wosnick, C. M. Mello, T. M. Swager, *J. Am. Chem. Soc.* **2005**, *127*, 3400. i) G. Angelini, C. Cusan, P. De Maria, A. Fontana, M. Maggini, M. Pierini, M. Prato, S. Schergna, C. Villani, *Eur. J. Org. Chem.* **2005**, 1884. j) Z. Gu, Y.-J. Bao, Y. Zhang, M. Wang, Q.-D. Shen, *Macromolecules* **2006**, *39*, 3125.

4 a) A. F. M. Kilbinger, A. P. H. J. Schenning, F. Goldoni, W. J. Feast, E. W. Meijer, *J. Am. Chem. Soc.* **2000**, *122*, 1820. b) A. P. H. J. Schenning, A. F. M. Kilbinger, F. Biscarini, M. Cavallini, H. J. Cooper, P. J. Derrick, W. J. Feast, R. Lazzaroni, Ph. Leclère, L. A. McDonnel, E. W. Meijer, S. C. J. Meskers, *J. Am. Chem. Soc.* **2002**, *124*, 1269. c) O. Henze, W. J. Feast, F. Gardebien, P. Jonkheijm, R. Lazzaroni, P. Leclère, E. W. Meijer, A. P. H. J. Schenning, *J. Am. Chem. Soc.* **2006**, *128*, 5923.

5 C. Xia, J. Locklin, J. H. Touk, T. Fulghum, R. C. Advincula, *Langmuir* **2002**, *18*, 955.

6 a) P. Jonkheijm, M. Fransen, A. P. H. J. Schenning, E. W. Meijer, *J. Chem. Soc., Perkin Trans. 2* **2001**, 1280. b) V. Urban, H. H. Wang, P. Thiyagarajan, K. C. Littrell, H. B. Wang, L. Yu, *J. Appl. Crystallogr.* **2000**, *33*, 645. c) H. Xiong, L. Qin, J. Sun, X. Zhang, J. Shen, *Chem. Lett.* **2000**, 586.

7 B. S. Gaylord, S. Wang, A. J. Heeger, G. C. Bazan, *J. Am. Chem. Soc.* **2001**, *123*, 6417.

8 a) R. Nonokawa, E. Yashima, *J. Am. Chem. Soc.* **2003**, *125*, 1278. b) E. Yashima, K. Maeda, O. Sato, *J. Am. Chem. Soc.* **2001**, *123*, 8159.

9 K. Akagi, G. Piao, S. Kaneko, K. Sakamaki, H. Shirakawa, M. Kyotani, *Science* **1998**, *282*, 1683.

10 a) R. B. Prince, L. Brunsveld, E. W. Meijer, J. S. Moore, *Angew. Chem., Int. Ed.* **2000**, *39*, 228. b) A. F. M. Kilbinger, A. P. H. J. Schenning, F. Goldoni, W. J. Feast, E. W. Meijer, *J. Am. Chem. Soc.* **2000**, *122*, 1820.

11 a) L. Brunsveld, E. W. Meijer, R. B. Prince, J. S. Moore, *J. Am. Chem. Soc.* **2001**, *123*, 7978. b) R. B. Prince, J. S. Moore, L. Brunsveld, E. W. Meijer, *Chem.—Eur. J.* **2001**, *7*, 4150.

12 a) P. Breccia, M. Van Gool, R. Pérez-Fernández, S. Martín-Santamaría, F. Gago, P. Prados, J. de Mendoza, *J. Am. Chem. Soc.* **2003**, *125*, 8270. b) H. Onouchi, T. Miyagawa, K. Morino, E. Yashima, *Angew. Chem., Int. Ed.* **2006**, *45*, 2381. c) S.-I. Sakurai, K. Okoshi, J. Kumaki, E. Yashima, *J. Am. Chem. Soc.* **2006**, *128*, 5650.

13 a) H. Fenniri, B.-L. Deng, A. E. Ribbe, *J. Am. Chem. Soc.* **2002**, *124*, 11064. b) A. Tanatani, M. J. Mio, J. S. Moore, *J. Am. Chem. Soc.* **2001**, *123*, 1792.

14 M. Antonietti, J. Conrad, A. Thünemann, *Macromolecules* **1994**, *27*, 6007; M. R. J. Vos, G. E. Jardl, A. L. Pallas, M. Breurken, O. L. J. van Asselen, P. H. H. Bomans, Ph. E. L. G. Leclère, P. M. Frederik, R. J. M. Nolte, N. A. J. M. Sommerdijk, *J. Am. Chem. Soc.* **2005**, *127*, 16768.

15 See for example: a) S. Tamaru, M. Takeuki, M. Sano, S. Shinkai, *Angew. Chem.* **2002**, *114*, 881. b) G. Mieden-Gundert, L. Klein, M. Fischer, F. Vögtle, K. Heuzé, J. L. Pozzo, M. Vallier, F. Fages, *Angew. Chem.* **2001**, *113*, 3266. c) U. Maitra, S. Mukhopadhyay, A. Sarkar, P. Rao, S. S. Indi, *Angew. Chem.* **2001**, *113*, 2341. d) F. S. Schoonbeek, J. H. van Esch, R. Hulst, R. M. Kellog, B. L. Feringa, *Chem.—Eur. J.* **2000**, *6*, 2633. e) R. Wang, C. Geiger, L. Chen, B. Swanson, D. G. Whitten, *J. Am. Chem. Soc.* **2000**, *122*, 2399. f) J. H. van Esch, B. L. Feringa, *Angew. Chem.* **2000**, *112*, 2351. g) P. Terech, R. G. Weiss, *Chem. Rev.* **1997**, *97*, 3133.

16 a) A. Ajayaghosh, S. J. George, V. K. Praveen, *Angew. Chem., Int. Ed.* **2003**, *42*, 332. b) W. Y. Huang, S. Matsuoka, T. K. Kwei, Y. Okamoto, *Macromolecules* **2001**, *34*, 7166. c) C. Geiger, M. Stanescu, L. Chen, D. G. Whitten, *Langmuir* **1999**, *15*, 2241. d) M. Grell, D. D. C. Bradley, X. Long, T. Chamberlain, M. Inbasekaran, E. P. Woo, M. Soliman, *Acta Polym.* **1998**, *49*, 439. e) T. Brotin, R. Utermöhlen, F. Fages, H. Boucas-Laurent, J. P. Desvergne, *J. Chem. Soc., Chem. Commun.* **1991**, 416. f) T. M. Swager, C. J. Gil, M. S. Wrighton, *J. Phys. Chem.* **1995**, *99*, 4886. g) A. Ajayaghosh, R. Varghese, S. J. George, C. Vijayakumar, *Angew. Chem., Int. Ed.* **2006**, *45*, 1141. h) K. Sugiyasu, N. Fujita, S. Shinkai, *Angew. Chem., Int. Ed.* **2004**, *43*, 1229. i) A. Ajayaghosh, R. Varghese, V. K. Praveen, S. Mahesh, *Angew. Chem., Int. Ed.* **2006**, *45*, 3261.

17 a) D. B. A. Rep, R. Roelfsema, J. H. van Esch, F. S. Schoonbeek, R. M. Kellogg, B. L. Feringa, T. T. M. Palstra, T. M. Klapwijk, *Adv. Mater.* **2000**, *12*, 563. b) F. S. Schoonbeek, J. H. van Esch, B. Wegewijs, D. B. A. Rep, M. P. de Haas, T. M. Klapwijk, R. M. Kellog, B. L. Feringa, *Angew. Chem., Int. Ed.* **1999**, *38*, 1393.

18 See for example: a) M. L. Bushey, A. Hwang, P. W. Stephens, C. Nickholls, *Angew. Chem., Int. Ed.* **2002**, *41*, 2828. b) M. P. Lightfoot, F. S. Mair, R. C. Pritchard, J. E. Warren, *Chem. Commun.* **1999**, 1945. c) V. Percec, C.-H. Ahn, T. K. Bera, G. Ungar, D. J. P. Yeardley, *Chem.—Eur. J.* **1999**, *5*, 1070.

19 See for example: a) W. Shu, S. Valiyaveetil, *Chem. Commun.* **2002**, 1350. b) J. J. van Gorp, J. A. J. M. Vekemans, E. W. Meijer, *J. Am. Chem. Soc.* **2002**, *124*, 14759. c) L. Brunsveld, H. Zhang, M. Glasbeek, J. A. J. M. Vekemans, E. W. Meijer, *J. Am. Chem. Soc.* **2000**, *122*, 6175. d) A. R. A. Palmans, J. A. J. M. Vekemans, E. E. Havinga, E. W. Meijer, *Angew. Chem., Int. Ed. Engl.* **1997**, *36*, 2648. e) R. Kleppinger, P. Lillya, C. Yang, *J. Am. Chem. Soc.* **1997**, *119*, 4097.

20 For a review see: a) G. G. Wallace, L. A. P. Kane-Maguire, *Adv. Mater.* **2002**, *14*, 953. b) S. B. Adeloju, G. G. Wallace, *Analyst* **1996**, *121*, 699. c) W. Schuhmann, *Mikrochim. Acta* **1995**, *121*, 1. d) P. N. Bartlett, P. R. Birkin, *Synth. Met.* **1993**, *61*, 15. e) For a review about bioelectronics see: I. Willner, E. Katz, *Angew. Chem., Int. Ed.* **2000**, *39*, 1180.

21 a) B. S. Gaylord, A. J. Heeger, G. C. Bazan, *J. Am. Chem. Soc.* **2003**, *125*, 896. b) K. P. R. Nilsson, O. Inganäs, *Nat. Mater.* **2003**, *2*, 419. c) H.-A. Ho, M. Boissinot, M. G. Bergeron, G. Corbeil, K. Doré, D. Boudreau, M. Leclerc, *J. Am. Chem. Soc.* **2003**, *125*, 896. d) S. Bernier, S. Garreau, M. Béra-Abérem,

C. Gravel, M. Leclerc, *J. Am. Chem. Soc.* **2002**, *124*, 12463. e) P. C. Ewbank, G. Nuding, H. Suenaga, R. D. McCullough, S. Shinkai, *Tetrahedron Lett.* **2001**, *42*, 155. f) L. Chen, D. W. McBranch, H.-L. Wang, R. Helgeson, F. Wudl, D. Whitten, *Proc. Natl. Acad. Sci. U.S.A.* **1999**, *96*, 12287.

22 A. Yassar, G. Horowitz, P. Valat, V. Wintgens, M. Hmyene, F. Deloffre, P. Srivastava, P. Lang, F. Garnier, *J. Phys. Chem.* **1995**, *99*, 9155.

23 M. Sundberg, O. Inganäs, S. Stafström, G. Gustafsson, B. Sjögren, *Solid State Commun.* **1989**, *71*, 435.

24 Ph. Leclère, M. Surin, O. Henze, P. Jonkheijm, F. Biscarini, M. Cavallini, W. J. Feast, A. F. M. Kilbinger, R. Lazzaroni, E. W. Meijer, A. P. H. J. Schenning, *J. Mater. Chem.* **2004**, *16*, 4452.

25 Ribbon-like fibrils are formed when **2** is deposited on silicon wafers or graphite. However, the present rod-like assemblies of **1** appear considerably more rigid and are more homogeneous in shape.

26 A similar value (381 nm) was obtained for **2** in the same solvent.

27 The shape and dimensions of the aggregates in solution were confirmed by preliminary SAXS and DLS experiments.

28 a) S. Hotta, K. Waragai, *Adv. Mater.* **1993**, *5*, 896. b) D. Fichou, *J. Mater. Chem.* **2000**, *10*, 571.

29 J. Cornil, D. Beljonne, J.-P. Calbert, J.-L. Brédas, *Adv. Mater.* **2001**, *13*, 1053.

30 C. Quattrocchi, R. Lazzaroni, J. L. Brédas, *Chem. Phys. Lett.* **1993**, *208*, 120.

31 The complex was formed in the presence of 2% v/v DMSO in water. It was therefore impossible to detect any low wavelength CD signal relative to the polypeptidic chain.

32 a) D. Zanuy, C. Alemán, S. Muñoz-Guerra, *Biopolymers* **2002**, *63*, 151. b) E. A. Ponomarenko, A. J. Waddon, D. A. Tirrell, W. J. Macknight, *Langmuir* **1996**, *12*, 2169. c) M. Tabet, V. Labroo, P. Sheppard, T. Sasaki, *J. Am. Chem. Soc.* **1993**, *115*, 3866.

33 The low intensity of the CD effect is attributed to the large distance between the oligothiophene segment and the chiral centers of the PLG, see e.g. D. B. Amabilino, E. Ramos, J.-L. Serrano, T. Sierra, J. Veciana, *J. Am. Chem. Soc.* **1998**, *120*, 9126.

34 D. Zanuy, C. Alemán, *Biopolymers* **1999**, *49*, 497.

35 a) E. Yashima, H. Goto, Y. Okamoto, *Macromolecules* **1999**, *32*, 7942. b) B. M. W. Langeveld-Voss, D. Beljonne, Z. Shuai, R. A. J. Janssen, S. C. J. Meskers, E. W. Meijer, J.-L. Brédas, *Adv. Mater.* **1998**, *10*, 1343.

36 P. S. Heeger, A. J. Heeger, *Proc. Natl. Acad. Sci. U.S.A.* **1999**, *96*, 12219.

37 a) J. Wang, D. Wang, E. K. Miller, D. Moses, G. C. Bazan, A. J. Heeger, *Macromolecules* **2000**, *33*, 5153. b) D. Wang, X. Gong, P. S. Heeger, F. Rininsland, G. C. Bazan, A. J. Heeger, *Proc. Natl. Acad. Sci. U.S.A.* **2002**, *99*, 49.

38 P. Samorì, V. Francke, T. Mangel, K. Müllen, J. Rabe, *Opt. Mater.* **1998**, *9*, 390.

39 S. L. Mayo, B. D. Olafson, W. A. Goddard, III, *J. Phys. Chem.* **1990**, *94*, 8897.

40 A. Gesquière, M. M. S. Abdel-Mottaleb, S. De Feyter, F. C. De Schryver, F. Schoonbeek, J. van Esch, R. M. Kellogg, B. L. Feringa, A. Calderone, R. Lazzaroni, J. L. Brédas, *Langmuir* **2000**, *16*, 10385.

41 M. C. Zerner, G. H. Loew, R. F. Kirchner, U. T. Mueller-Westerhoff, *J. Am. Chem. Soc.* **1980**, *102*, 589.

42 S. Kotani, K. Shiina, K. Sonogashira, *J. Organomet. Chem.* **1992**, *429*, 403.